

# Thermal regime and gravitational instability of multi-layered continental crust: implications for the buoyant exhumation of high-grade metamorphic rocks

TARAS V. GERYA<sup>1,2,\*</sup>, LEONID L. PERCHUK<sup>1,3</sup>, WALTER V. MARESCH<sup>2</sup>,  
ARNE P. WILLNER<sup>2</sup>, DIRK D. VAN REENEN<sup>4</sup> and C. ANDRE SMIT<sup>4</sup>

<sup>1</sup>Institute of Experimental Mineralogy, Russian Academy of Sciences, Chernogolovka, Moscow district, 142432, Russia

<sup>2</sup>Institut für Geologie, Mineralogie und Geophysik, Ruhr-Universität Bochum, 44780 Bochum, Germany

<sup>3</sup>Department of Petrology, Moscow State University, Vorobievsky Gory, Moscow, 119899 Russia

<sup>4</sup>Department of Geology, Rand Afrikaans University, Auckland Park, South Africa

**Abstract:** Large-scale crustal thickening by tectonic and/or magmatic processes can lead to various complex patterns of multi-layered continental crust. It is well-known from one-dimensional thermal modeling that variations in total crustal thickness, mantle lithospheric thickness, thermal conductivities of the crust, and bulk radiogenic heat production of the crust will lead to variable geotherms in such heterogeneously stacked crust. By systematically changing the above parameters, we illustrate that variations on the order of 100-500°C will result at a depth of 30 km. Specifically, we show that geotherms are also strongly dependent on the *pattern* of vertical interlayering. Assuming a crustal structure composed of idealized granodioritic/gabbroic or granodioritic/dioritic compositional layer sequences, it can be shown that such gravitationally unstable, stacked, multi-layered continental crust can lead to temperature variations in geotherms of comparable magnitude as for the above parameters. Geotherms exhibiting the highest temperatures at a given depth are characteristic for gravitationally unstable structures in which the bulk of the granodioritic rocks underlie dioritic or gabbroic rocks. Thus a strong positive correlation between temperature and the estimated degree of gravitational instability of the multilayered crust is indicated. It is argued that the lowering of the viscosity of rocks with increasing temperature after tectonic or magmatic stacking will set the stage for processes of gravitational redistribution and buoyant exhumation of high-grade metamorphic rocks. Prograde changes in metamorphic mineral assemblages and partial melting during thermal relaxation after stacking provide positive feed-back mechanisms to enhance the possibility of gravitational redistribution. In keeping with the published results of Babeyko & Sobolev (2001) and Arnold *et al.* (2001), we find that gravitational overturn can be triggered only when external tectonic forces are active after stacking. Time-scales of 10 to 100 Myr are indicated for differential movement of rock masses on a kilometer-scale when the viscosity of crustal rocks is lowered to  $n \times 10^{21}$  Pa·s, but may be considerably less if zones of tectonic weakness in the crust lead to a further local decrease in effective rock viscosity.

**Key-words:** thermal modeling, layered continental crust, gravitational instability, crustal diapirism.

## Introduction

Theoretical modeling is an extremely useful tool for studying large-scale crustal geodynamic processes of various types (*e.g.*, Turcotte & Schubert, 1982; Cloos, 1982; England & Thompson, 1984, 1986; Shi & Wang, 1987; Buntebarth, 1991; Ruppel & Hodges, 1994; Henry *et al.*, 1997; Le Pichon *et al.*, 1997; Midgley & Blundell, 1997; Ellis *et al.*, 1999), particularly when the results are considered in terms of the pressure-temperature-time paths of the rocks involved in a particular geodynamic setting (*e.g.*, England & Thompson, 1984; Ruppel & Hodges, 1994; Gerya *et al.*, 2000a and b; Willner *et al.*, 2002). Although many such studies have primarily focussed on the early collisional stages of various crustal geodynamic

scenarios, which can be considered in terms of *external* driving forces, it is clear that in many cases crustal structures must result that are inherently gravitationally unstable. Given the appropriate rheological conditions (*e.g.*, Ramberg, 1981; Ranalli, 1995), *internal* gravitational driving forces should lead to deformation and diapiric crustal redistribution during late, exhumation-related tectonic phases. Indeed, processes of gravitational redistribution of crustal rocks have been considered by some authors to be among the most important geodynamic factors controlling the evolution of high-grade metamorphic complexes (*e.g.*, Belousov, 1989; Perchuk, 1989, 1991; Perchuk *et al.*, 1992, 1996, 1999, 2000a and b; Weinberg & Schmeling, 1992; Dirks, 1995; Bittner & Schmeling, 1995; Gerya *et al.*, 2000a and b, 2001).

\*E-mail: Taras.Gerya@ruhr-uni-bochum.de

Gerya *et al.* (2001) summarized some of the various ways in which gravitationally unstable continental crust has been suggested to develop. Not all of these processes must necessarily be directly related to collision. The development of lithological density contrasts has been ascribed to the superposition or injection of dense basic magmas (*e.g.*, Ramberg, 1981; Perchuk, 1989, 1992) or to crustal anatexis and granitization (Ramberg, 1981; Perchuk, 1989; Bittner & Schmeling, 1995). Nevertheless, it is primarily collision that will lead to either homogeneous thickening or multiple stacking of initially stable crustal profiles (*e.g.*, Ramberg, 1981; Turcotte & Schubert, 1982; England & Thompson, 1984; De Wit & Ashwal, 1997; Krohe, 1998; Le Pichon *et al.*, 1997). Gravitational instability can be due either to primary density contrasts in stacked crust or to inversions of rock densities caused by reequilibration leading to either partial melting (at relatively high water fugacities) or to a granulite-facies overprint with the production of mineral assemblages of comparatively lower density (Gerya *et al.*, 2001).

England & Thompson (1984) have already shown that the internal layering of continental crust, reflecting a particular process of crustal thickening, decisively controls crustal thermal structure if the radiogenic heat supply from the crust and mantle, the thermal conductivities and the rates and duration of erosion are kept constant. For instance, England & Thompson (1984) demonstrated that regions thickened by crustal-scale thrusting (*e.g.*, a four-layered crust) should be characterized at a given depth by considerably higher ( $\sim 100^\circ\text{C}$ ) temperatures than regions of homogeneously thickened two-layered crust (see also Le Pichon *et al.*, 1997). In contrast to the homogeneously thickened crust, the stacked crust has a gravitationally unstable internal structure, because lower crustal rocks of relatively high density are thrust over upper crustal rocks of relatively lower density.

In the present paper we study in a more systematic approach the influence of the internal structure of multiply and variously layered/stacked continental crust on its thermal regime, and assess the question of resulting gravitational instability and its implications for the exhumation process of high-grade metamorphic rocks.

## Thermal modeling of steady-state geotherms

### Physical model

We use a 1D model of the continental crust and upper mantle (Turcotte & Schubert, 1982; England & Thompson, 1984; Le Pichon *et al.*, 1997) in which non-convecting lithosphere is underlain by convecting asthenosphere. We take boundary conditions for the lithosphere of  $T = 25^\circ\text{C}$  at the surface and  $T = 1300^\circ\text{C}$  at its base. We assume

- that the decay of radiogenic elements from the continental crust and the heat transferred to the bottom of the crust from the mantle are the two sources of heat;
- that heat flow from the mantle is controlled by the thickness of mantle lithosphere;
- that heat transfer occurs by conduction in the vertical direction only;

and we take into account

- that rocks have a temperature-dependent thermal conductivity (*e.g.*, Clauser & Huenges, 1995).

With the above constraints, a set of steady-state temperature profiles (*i.e.*, geotherms) can be calculated for multi-layered continental crust according to

$$\partial(k\partial T/\partial z)/\partial z + Q = 0, \quad (1)$$

where  $z$  is depth in m;  $T$  is temperature, K;  $k$  is thermal conductivity of the medium, W/(m·K); and  $Q$  is radiogenic

Table 1. The basic set of standard model parameters assumed for calculations; in brackets the range of individual parameter variations explored while holding all other parameters constant.

Physical parameters	Continental Crust			Mantle	Reference
	granodioritic rocks	dioritic rocks	gabbroic rocks	Lithosphere ultramafic rocks	
Thermal conductivity, $k$ ( $\text{W}\cdot\text{m}^{-1}\cdot\text{K}^{-1}$ )	$0.64 + \frac{807}{T+77}$ ( $\pm 30\%$ )	$0.91 + \frac{641}{T+77}$ *	$1.18 + \frac{474}{T+77}$ ( $\pm 30\%$ )	$0.73 + \frac{1293}{T+77}$	Le Pichon <i>et al.</i> , (1997); England & Thompson (1984); Clauser & Huenges (1995)
Bulk radiogenic heat production, $Q$ ( $\text{W}\cdot\text{m}^{-3}$ )	$2 \times 10^{-6}$ ( $1.0 - 3.0 \times 10^{-6}$ )	$5 \times 10^{-7}$ ( $3.0 - 7.0 \times 10^{-7}$ )	$2.5 \times 10^{-7}$ ( $1.5 - 3.5 \times 10^{-7}$ )	$2.2 \times 10^{-8}$	Le Pichon <i>et al.</i> , 1997; England & Thompson (1984); Turcotte & Schubert (1982)
Density, $\rho$ ( $\text{kg}\cdot\text{m}^{-3}$ )	2800	2900	3000	3300	Turcotte & Schubert (1982)
Thickness, km	25 (15 - 35)	25 (15 - 35)	25 (15 - 35)	100 (50-150)	Le Pichon <i>et al.</i> (1997), England & Thompson, (1984), Turcotte & Schubert (1982)

\* thermal conductivity of dioritic rocks is taken as the average for granodioritic and gabbroic rocks.

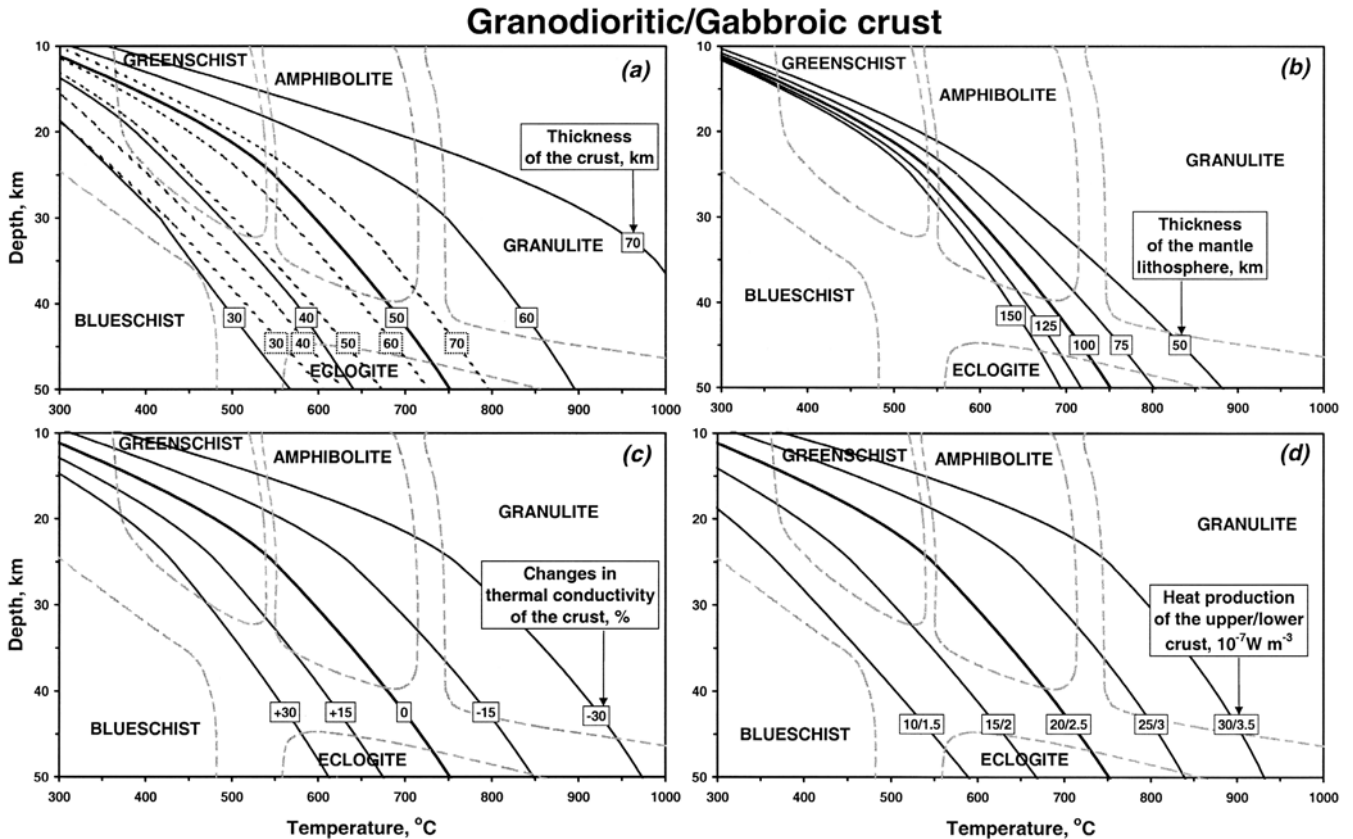


Fig. 1. Steady-state temperature distribution in a thickened granodioritic/gabbroic crust, calculated on the basis of the standard parameters given in Table 1. Each panel shows the influence of varying independently (a) the total thickness of the crust with equally thick layers of upper granodioritic and lower gabbroic rocks, (b) the thickness of the mantle lithosphere, (c) the thermal conductivity of the crust, and (d) the bulk heat production within the crust. For comparison, geotherms calculated at constant thermal conductivity of upper crust ( $3.0 \text{ W}\cdot\text{m}^{-1}\cdot\text{K}^{-1}$ ), lower crust ( $2.6 \text{ W}\cdot\text{m}^{-1}\cdot\text{K}^{-1}$ ) and mantle ( $3.0 \text{ W}\cdot\text{m}^{-1}\cdot\text{K}^{-1}$ ) (England & Thompson, 1984; Le Pichon *et al.*, 1997) are given as dotted lines in (a). A simplified facies scheme from Yardley (1989) is shown for orientation.

heat production in the medium,  $\text{W}/\text{m}^3$ . For the lithospheric layer boundaries, equation (1) was combined with the condition of equal heat flow,

$$k_A(\partial T/\partial z)_A = k_B(\partial T/\partial z)_B \quad (2)$$

where  $k_A$  and  $k_B$  are the heat conductivities of adjacent layers A and B, respectively, and  $(\partial T/\partial z)_A$  and  $(\partial T/\partial z)_B$  are related to the adjacent layers at their contact.

The steady-state temperature distribution within the lithosphere in our model is controlled by the following physical parameters: (A) overall thickness of the crust, (B) thickness of mantle lithosphere, (C) thermal conductivity of the crust, (D) bulk radiogenic heat supply within the crust, and (E) the distribution of rock layers of different heat productivity within the crust.

We have studied two types of initial *crustal layering* (e.g., Le Pichon *et al.*, 1997): (1) intercalation of rocks of granodioritic and gabbroic bulk composition on the one hand, and (2) intercalation of rocks of granodioritic and dioritic bulk composition on the other. Table 1 lists the basic set of standard model parameters we have assumed, as well as the range of individual parameter variations we

have explored while holding all other parameters constant. As the *standard lithosphere* we use a 50 km, two-layered, homogeneously thickened crust underlain by 100 km of mantle lithosphere. The vertical structure of the *standard crust* is defined by an upper crust composed of 25 km of rocks of granodioritic bulk composition and a lower crust composed of 25 km of either gabbroic or dioritic bulk composition (compare with Le Pichon *et al.*, 1997).

## Results of modeling

Figures 1 and 2 illustrate the variations in calculated temperature distributions that result as a function of isolated, independent changes in the model parameters summarized in Table 1. These results are comparable with those reported by England & Thompson (1984) and Le Pichon *et al.* (1997), and indicate that the realistic systematic variations assumed in Table 1 in total crustal thickness, mantle lithospheric thickness, thermal conductivities of the crust, and bulk radiogenic heat production of the crust will lead to variations in the temperatures of steady-state geotherms on the order of 100–500°C at 30 km depth. However, the more realistic temperature-dependent thermal conductivities intro-

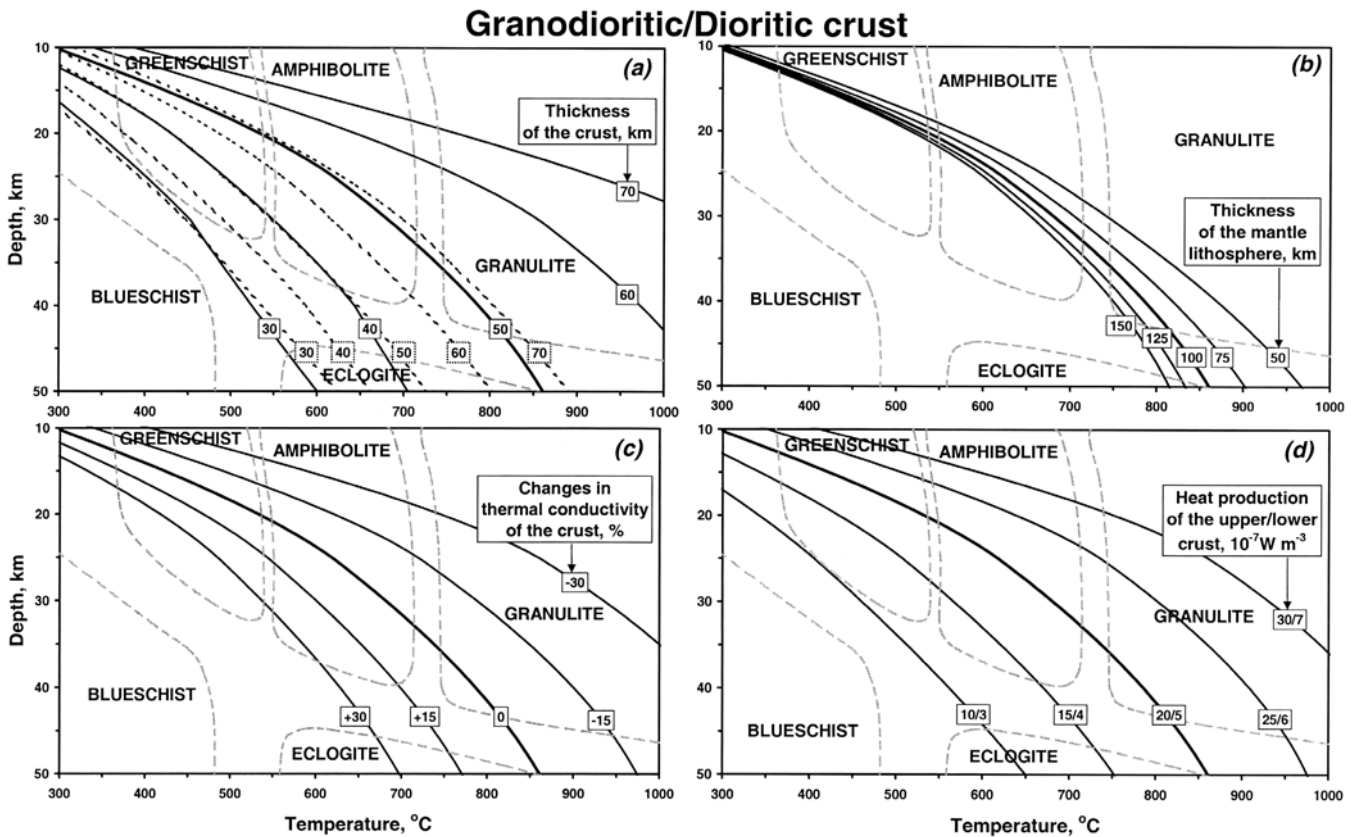


Fig. 2. Steady-state temperature distribution in a thickened granodioritic/dioritic crust, calculated on the basis of the standard parameters given in Table 1. Each panel shows the influence of varying independently (a) the total thickness of the crust with equally thick layers of upper granodioritic and lower dioritic rocks, (b) the thickness of the mantle lithosphere, (c) the thermal conductivity of the crust, and (d) the bulk heat production within the crust. For comparison, geotherms calculated at constant thermal conductivity of upper crust ( $3.0 \text{ W m}^{-1} \text{ K}^{-1}$ ), lower crust ( $2.6 \text{ W m}^{-1} \text{ K}^{-1}$ ) and mantle ( $3.0 \text{ W m}^{-1} \text{ K}^{-1}$ ) (England & Thompson, 1984; Le Pichon *et al.*, 1997) are given as dotted lines in (a). A simplified facies scheme from Yardley (1989) is shown for orientation.

duced in this study (Table 1) produce a systematic 100–300°C increase in calculated lower crustal temperatures and a more concave shape of the geotherms (Fig. 1a, 2a) in comparison to models based on a constant thermal conductivity of crustal rocks (*e.g.*, Turcotte & Schubert, 1982; England & Thompson, 1984; Le Pichon *et al.*, 1997).

Figure 3 demonstrates the thermal effects of different patterns of vertical structuring of the granodioritic/gabbroic or granodioritic/dioritic crust while retaining a 1:1 volume ratio between the two respective bulk-compositional layer types (*i.e.*, a constant bulk radiogenic heat supply within the crust) and a constant total crustal thickness of 50 km. The structural models 1 to 7 for the crust in Fig. 3 represent a continuous increase of the degree of gravitational instability of the crust from a completely stable to the most unstable geometry. The degree of gravitational instability clearly correlates positively with the higher temperature calculated at a given depth for the corresponding steady-state geotherm. This correlation documents the net shift of the higher-heat-generating units toward greater depths. The tested models illustrate an idealized progressive scheme and need not in detail be directly related to an actual, specific process of crustal thickening.

The models are applicable to any type of geodynamic process leading to specific contrasts and distribution patterns in density (*cf.* Introduction). Unstable crustal profiles of this type may be produced by magmatic and tectonic processes such as:

- regional stacking of continental crust during collision (*e.g.*, England & Thompson, 1984; Le Pichon *et al.*, 1997; Krohe, 1998; Arnold *et al.*, 2001), creating a potentially unstable thickened crust in areas with initially stable crustal profiles (*e.g.* double- and triple-stacked crust, see models 2 and 3 in Fig. 3).
- medium-scale (100–4000 m), rhythmic interlayering of rocks of different densities within the crust (*e.g.*, Perchuk, 1989), which has been suggested to lead to the growth of regional diapirs, due to the dynamic interaction of low density rocks during gravitational redistribution processes (Perchuk *et al.*, 1992) (see model 4 in Fig. 3);
- invasion of basic magmas, either in the form of huge quantities of basic melts pouring out on the top of continental crust (*e.g.*, plateau basalts, greenstone belts) or injected as sills, dykes and massive layered intrusions within continental crust (*e.g.*, Ramberg, 1981) (see models 5–7 in Fig. 3);



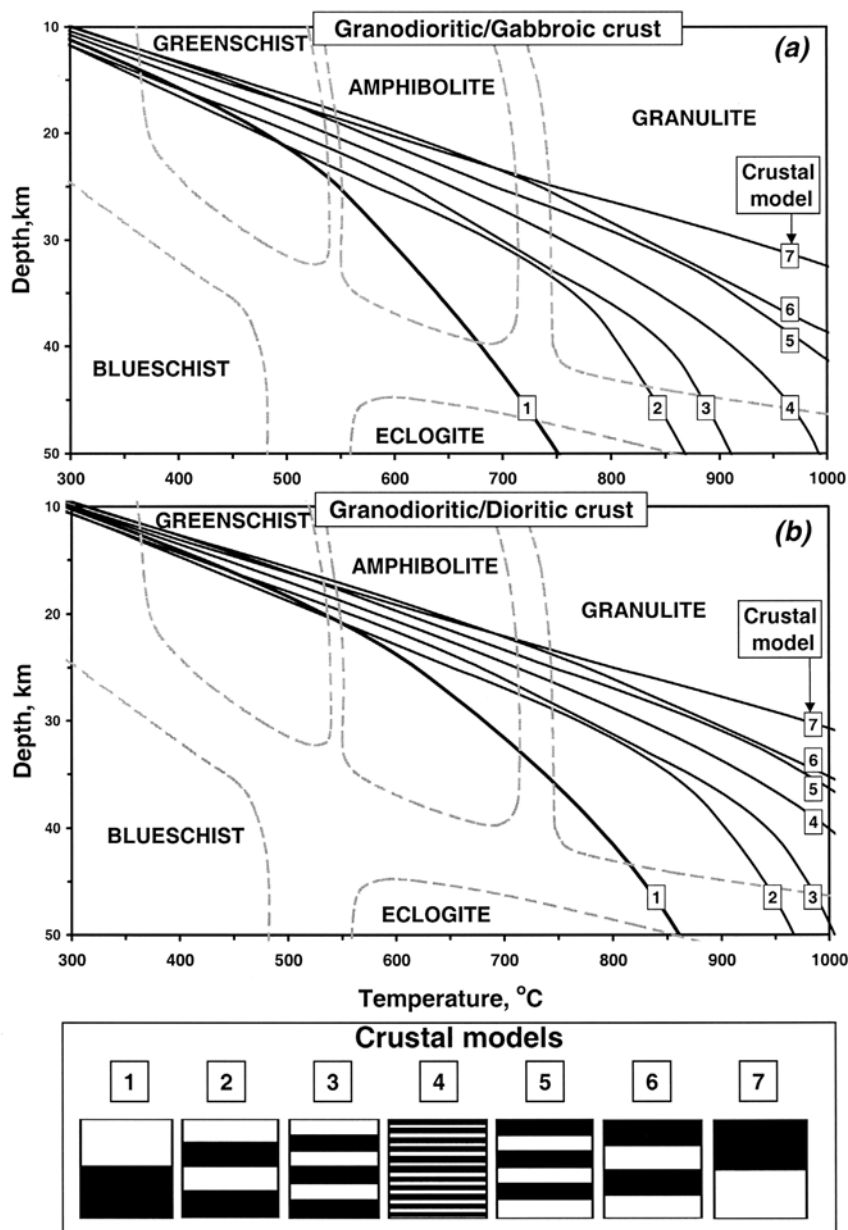


Fig. 3. Steady-state geotherms calculated for various types of restructured granodioritic/gabbroic (a) or granodioritic/dioritic (b) crust, retaining a 1:1 volume ratio between the two respective bulk-compositional layer types (*i.e.*, a constant bulk radiogenic heat supply within the crust) and a constant total crustal thickness of 50 km. All other standard parameters as in Table 1. Crustal models indicate distribution of granodioritic (white) and gabbroic or dioritic (black) layers. A simplified facies scheme from Yardley (1989) is shown for orientation.

The highest temperatures for a given depth in Fig. 3 are indicated for gravitationally unstable structures in which the bulk of the granodioritic rocks underlie dioritic or gabbroic rocks (*e.g.*, models 6 and 7 in Fig. 3). The calculated shifts in steady-state geotherms caused by such variations in the internal geometry of the crust are considerable. In the case of model 7 the temperature is about 300°C higher at a depth of 30 km than that calculated with model 1 (Fig. 3). *These shifts are thus of the same order of magnitude as those caused by variations in other model parameters (Fig. 1 and 2) usually taken into account.* For example, the change of vertical structure of the crust from model 1 to model 7 produces almost the same effect on a steady-state geotherm as a *twofold* increase in the bulk radiogenic heat production within the standard two-layered crust (*cf.* geotherms 15/2 and 30/3.5 in Fig. 1d).

The geodynamic processes leading to gravitationally unstable crust can be considered to be geologically instantaneous. However, although the steady-state geotherms in Fig. 1 and 2 represent thermal structures that the stacked crust will initially strive to attain, it remains to be explored to what degree late-orogenic relaxation will affect the thermal evolution of such gravitationally unstable crustal systems.

## Geodynamic implications

### Degree of gravitational instability of the crust

As follows from Fig. 3, the calculated increase in temperature at a given depth caused by variations in the vertical structure of the crust correlates directly with an

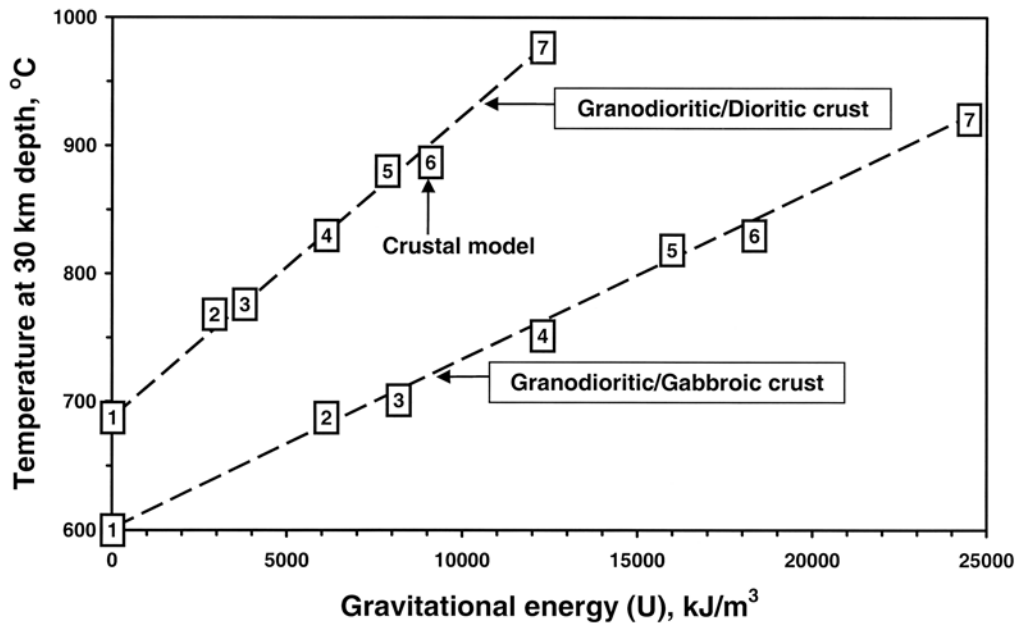


Fig. 4. Correlation of steady-state temperature at 30 km depth with gravitational energy,  $U$ , as calculated for different crustal models (see Fig. 3) according to Equation 3.

increase in the degree of gravitational instability of the crust. This correlation can be quantified in terms of the maximum internal gravitational energy released by gravitational redistribution. For any given density profile, the degree of gravitational instability can be estimated by comparison with a gravitationally stable “ordered” profile (model 1 in Fig. 3), characterized by identical volume ratios of rocks of different density, in which the density of the crust does not decrease with depth. The maximum internal gravitational energy,  $U$ , of the crust is given by

$$U = \frac{g}{h} \int_{z=0}^h [\rho(z) - \rho_o(z)] (h - z) dz, \quad (3)$$

where  $U$  is in  $J/m^3$ ;  $h$  is the thickness of the crust, m;  $\rho(z)$  and  $\rho_o(z)$  are given and “ordered” density profiles with depth  $z$ , respectively;  $g = 9.81 \text{ m}\cdot\text{s}^{-2}$  is the acceleration of gravity.  $U$  is here calculated using a standard rock density as listed in Table 1 and does not include the thermally induced density variations (*i.e.*, P-T-dependent changes in mineral assemblages, compressibilities and thermal expansion of individual minerals) discussed by Gerya *et al.* (2001).

Figure 4, calculated on the basis of Eqn. (3), shows a strong positive correlation between the gravitational energy (*i.e.*, degree of gravitational instability) of the crust  $U$  and temperatures at 30 km crustal level. Thus, the intercalation of rocks with different densities and rates of radiogenic heat production leads to a strong correlation between gravitational and thermal structures. This relationship reflects the general negative correlation for rocks between radiogenic heat production and  $\text{SiO}_2$  content on the one hand and density on the other.

#### Late orogenic thermal and metamorphic evolution of the crust

Steady-state geotherms calculated for gravitationally unstable crust (Fig. 3) will reflect the corresponding

crustal thermal structure towards which the thickened crust will evolve after the geodynamic event and during the late-orogenic, non-steady stage. Such thermal modeling has already been presented in the literature, considering both constant (*e.g.*, England & Thompson, 1984; Le Pichon *et al.*, 1997) and temperature-dependent (Arnold *et al.*, 2001) thermal conductivity and heat capacity of crustal rocks. The effect of partial melting was considered by Arnold *et al.* (2001). These models, however, do not explore the effects of the metamorphic phase transformations that will proceed with increasing temperature, consuming potentially significant amounts of heat (*e.g.*, Gerya *et al.*, 2001).

To account for the possible thermal effects of phase transformations under melt-absent conditions, we used 1D thermal modeling combined with a Gibbs free energy minimization approach. The latter procedure, following Gerya *et al.* (2001), was used to calculate equilibrium assemblages and compositions of minerals for a given pressure, temperature and rock composition. The density,  $\rho$ , of rock was then calculated as the ratio of the sum of the molar masses to the sum of the molar volumes of the constituent minerals, where each mass and volume is weighted by the molar abundance of the mineral in the rock. A similar procedure was also used to calculate the enthalpy of the rock. P-T dependent enthalpy,  $H$ , and molar volume,  $V$ , of the phases in equilibrium mineral assemblages were calculated *via* the Gibbs potential,  $G$ , using the thermodynamic relations  $V = \partial G / \partial P$  and  $H = G - T \cdot \partial G / \partial T$  and a numerical differentiation procedure. Enthalpy and density were tabulated for  $T = 25\text{--}1000^\circ\text{C}$  (at  $5^\circ\text{C}$  intervals) and  $P = 1\text{--}14,000$  bars (at intervals of 100 bars). Thermodynamic data for minerals and aqueous fluid were taken from the internally consistent database of Holland & Powell (1998). Mixing models of solid solutions consistent with this database were taken from the literature (Holland & Powell, 1998; Holland *et al.*, 1998; Powell & Holland, 1999; Dale *et al.*, 2000).

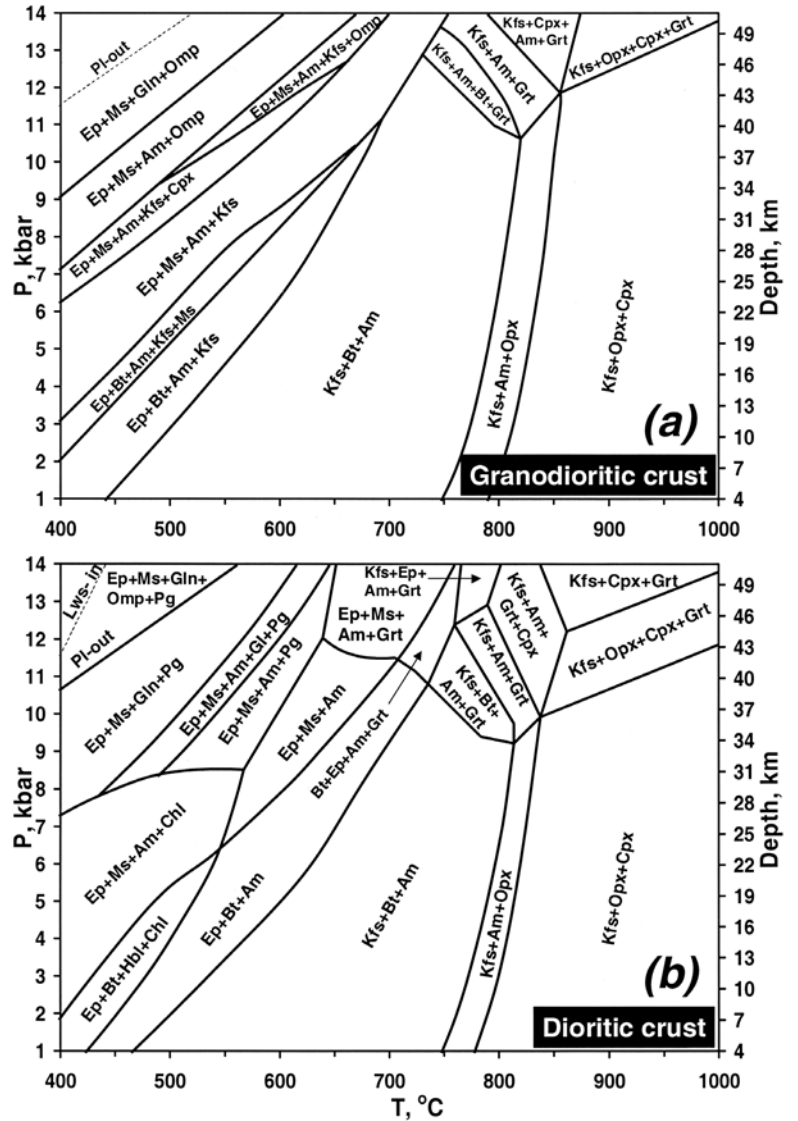


Fig. 5. Simplified petrogenetic grids calculated for a crust of granodioritic (a) and dioritic (b) composition. Quartz, plagioclase (otherwise specified) and Fe-Ti oxides are present in all mineral assemblages. Abbreviations of mineral names are after Kretz (1983).

Chemical compositions of granodioritic and andesitic crust were chosen according to McLennan (1992). To simulate melt-absent conditions, a lowered water activity was assumed at temperatures above 630°C according to the following empirical equation (Gerya *et al.*, 2001)

$$a_{\text{H}_2\text{O}} = 1.0 - [1.2(T_{\text{k}} + 20 - t_1)/(t_2 - t_1)]^{0.865}, \quad (4)$$

where  $t_1 = 877 + 160/(P_{\text{kbar}} + 0.348)^{0.75}$  and  $t_2 = 1262 + 9P_{\text{kbar}}$ ,  $0.1 < a_{\text{H}_2\text{O}} < 1.0$ .

Further details on this Gibbs energy minimization procedure and examples of calculations are given in Gerya *et al.* (2001).

With the above constraints, a set of time-dependent temperature profiles (*i.e.*, geotherms) were calculated for the case of thermal relaxation of double-stacked crust according to

$$\partial T / \partial t = \rho^{-1} C_p^{-1} [\partial(k \partial T / \partial z) / \partial z + Q], \quad (5)$$

where  $t$  is time,  $s$ ;  $\rho$  is equilibrium density of rock,  $\text{kg}/\text{m}^3$ ;  $C_p$  is the effective isobaric heat capacity that accounts for the thermal effects of phase transformations,  $\text{J}/\text{kg}$  (calculated numerically *via* tabulated enthalpy,  $H$ , using the  $C_p = \partial H / \partial T$  relation). Figure 5 shows equilibrium phase diagrams calculated at  $T = 400\text{--}1000^\circ\text{C}$  and  $P = 1\text{--}14$  kbar for crust of granodioritic and dioritic compositions (McLennan, 1992). To calculate the effective heat capacity and density of the crust it was assumed that complete reequilibration of a mineral assemblage is reached at a temperature above 400°C. At lower temperatures the heat capacity and the density were calculated for the assemblage stable at  $T = 400^\circ\text{C}$  and given pressure (with 1 kbar as lower pressure limit). To solve equation (5) we used a numerical modeling approach based on the implicit finite differences method. We also used a time-step limitation to ensure  $< 1^\circ\text{C}$  changes in temperature for each calculation step. The method of modeling and tests of the numerical code are discussed by Gerya *et al.* (2000).

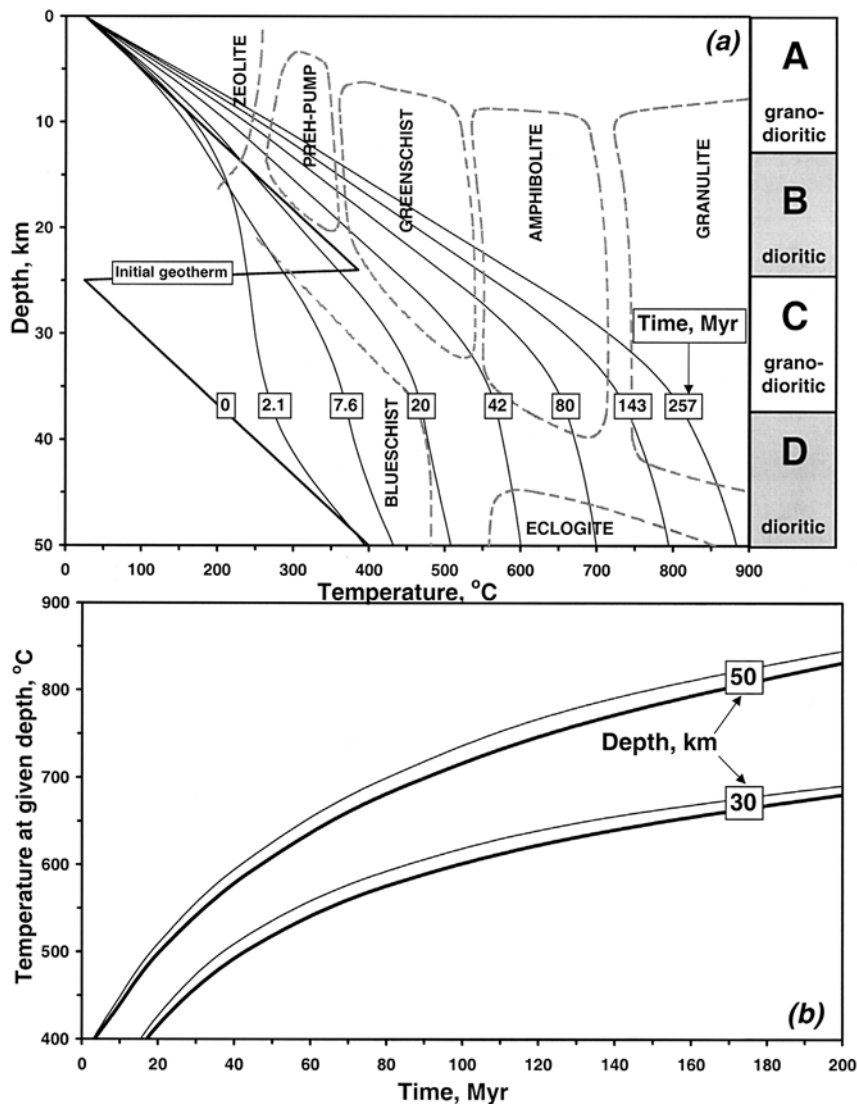


Fig. 6. Results of 1D modeling of the evolution of crustal temperatures in a double-stacked crust composed of granodioritic and dioritic rocks (Model 2 in Fig. 3b). (a) - evolution of the geothermal gradient with time when considering metamorphic phase transformations within the crust (see Fig. 5). A simplified facies scheme from Yardley (1989) is shown for orientation. (b) - changes in temperature at 30 and 50 km depth during the thermal evolution of a double-stacked crust: thick lines - thermal relaxation considering concomitant metamorphic phase transformations (Fig. 5), thin lines - thermal relaxation without associated phase transformations (modal compositions of granodioritic and dioritic crust correspond to the Qtz+Pl+Kfs+Bt+Am assemblage at 700°C and 7 kbar).

Figure 6a shows the results of modeling the late-orogenic evolution of the thermal profile in double-stacked continental crust composed of rocks of granodioritic and dioritic compositions. Geometry and boundary conditions correspond to crustal model 2 in Fig. 3b. Figure 6b demonstrates the influence of phase transformations on the evolution of the thermal profile with time: the consumption of heat related to prograde metamorphic reactions produces only a relatively small (10–20°C) systematic decrease in crustal temperatures at a given time, compared to the results calculated for a constant modal composition of the rock (compare thin and thick lines in Fig. 6b). Within the tabulated pressure (1–14,000 bars) and temperature (25–1000°C) range, the calculated average values of effective isobaric heat capacity including effects of metamorphic phase transformations are equal to 1162 J/kg for granodioritic and 1198 J/kg for dioritic crust. These values are *ca.* 10% higher than those (1091 J/kg for granodioritic and 1089 J/kg for dioritic crust) averaged in the tabulated pressure and

temperature range for a constant modal composition of rocks that corresponds to the Qtz+Pl+Kfs+Bt+Am assemblage equilibrating at 700°C and 7 kbar.

Calculated changes in the density and viscosity structure of the crust during the late orogenic evolution are shown in Fig. 7: prograde metamorphic reactions and increases in lower crustal temperatures toward high-grade amphibolite and granulite facies conditions (Fig. 6a) result in significant lowering of both density and viscosity of the buried granodioritic crust, thus creating even more favorable conditions for triggering processes gravitational redistribution (Gerya *et al.*, 2001).

#### Rheological constraints on gravitational redistribution

The possibility of gravitational redistribution within an unstable crust strongly depends on its effective viscosity, which decreases exponentially with increasing temperature (*e.g.* Turcotte & Schubert, 1982; Ranalli, 1995), and therefore varies significantly with depth and the effective



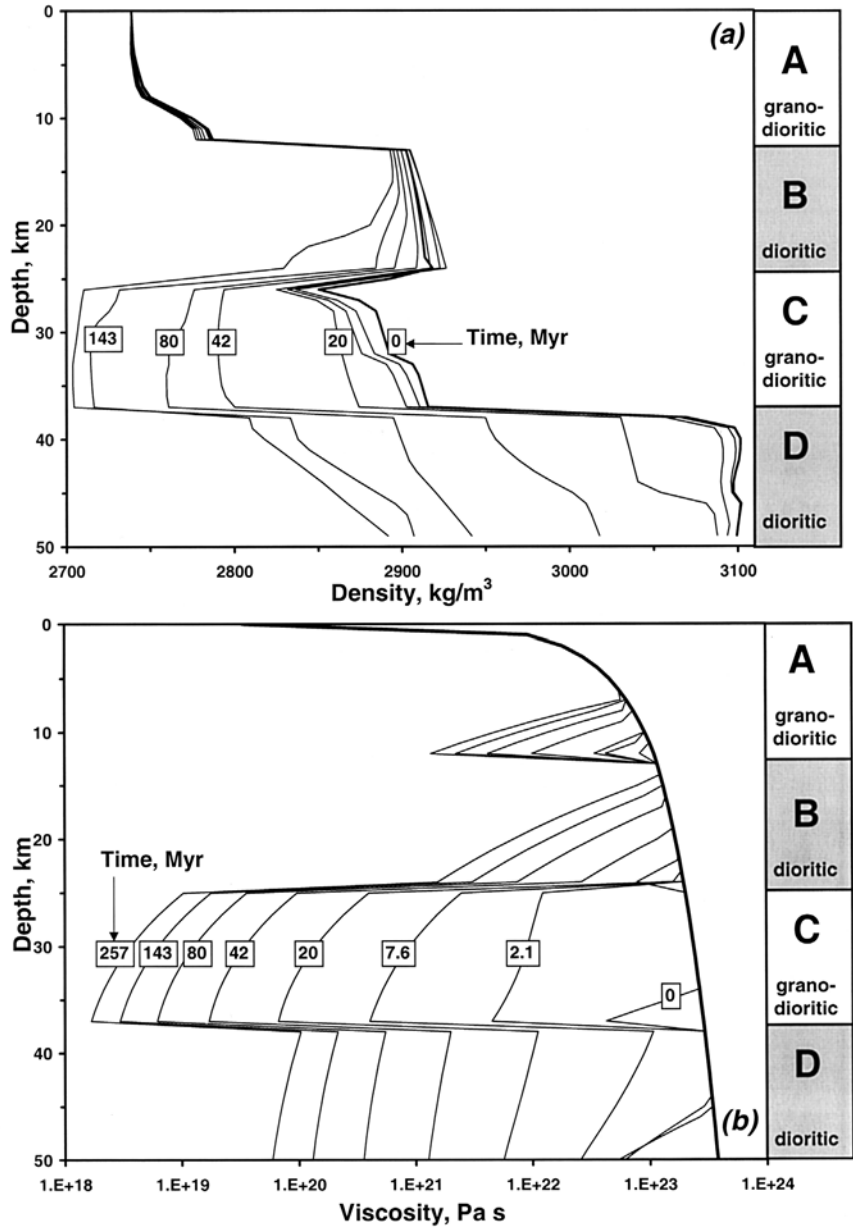


Fig. 7. Evolution of the vertical density (a) and viscosity (b) profile for a double-stacked crust (Model 2 in Fig. 3b), calculated for the corresponding thermal evolution shown in Fig. 6a. Changes in crustal density in (a) are related to metamorphic phase transformations (Fig. 5). The viscosity in (b) is calculated at a strain rate of  $10^{-15} \text{ s}^{-1}$  from experimentally determined rheological parameters given in Ranalli (1995); brittle-ductile transition (thick line) is calculated as “Mohr-Coulomb viscosity” (Schott & Schmeling, 1998) at a strain rate of  $10^{-15} \text{ s}^{-1}$  after Byerlee’s law (Brace, 1980).

geothermal gradient. Figure 7b illustrates the evolution of the viscosity profile for a double-stacked crust (model 2 in Fig. 3) during thermal relaxation, calculated using experimentally calibrated rheological criteria formulated according to Ranalli (1995) as

$$\epsilon = A_D \sigma^n \exp(-E/RT), \tag{6}$$

$$\eta = 10^6 \sigma / (2\epsilon) \tag{7}$$

where  $\eta$  is viscosity, Pa-s;  $\epsilon$  is strain rate,  $\text{s}^{-1}$ ;  $\sigma$  is stress, Mpa;  $E$  is activation energy,  $\text{kJ mol}^{-1}$ ;  $A_D$  is a material constant,  $\text{MPa}^{-n}\text{s}^{-1}$ , where  $n$  is a power-law constant;  $R$  is the gas constant. Data for granodioritic (wet granite rheology) and dioritic (quartz diorite rheology) crust in

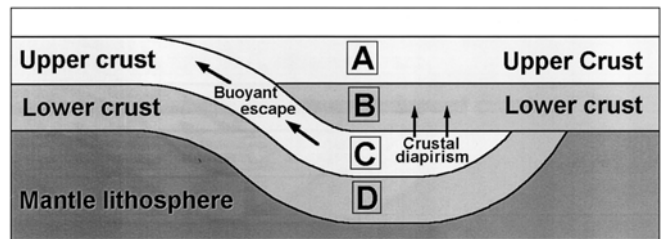


Fig. 8. Schematic geometry of double-stacked crust (e.g., Shemenda, 1993; Le Pichon *et al.*, 1997) and processes of gravitational redistribution contributing to the buoyant exhumation of buried upper crustal rocks (Layer C).

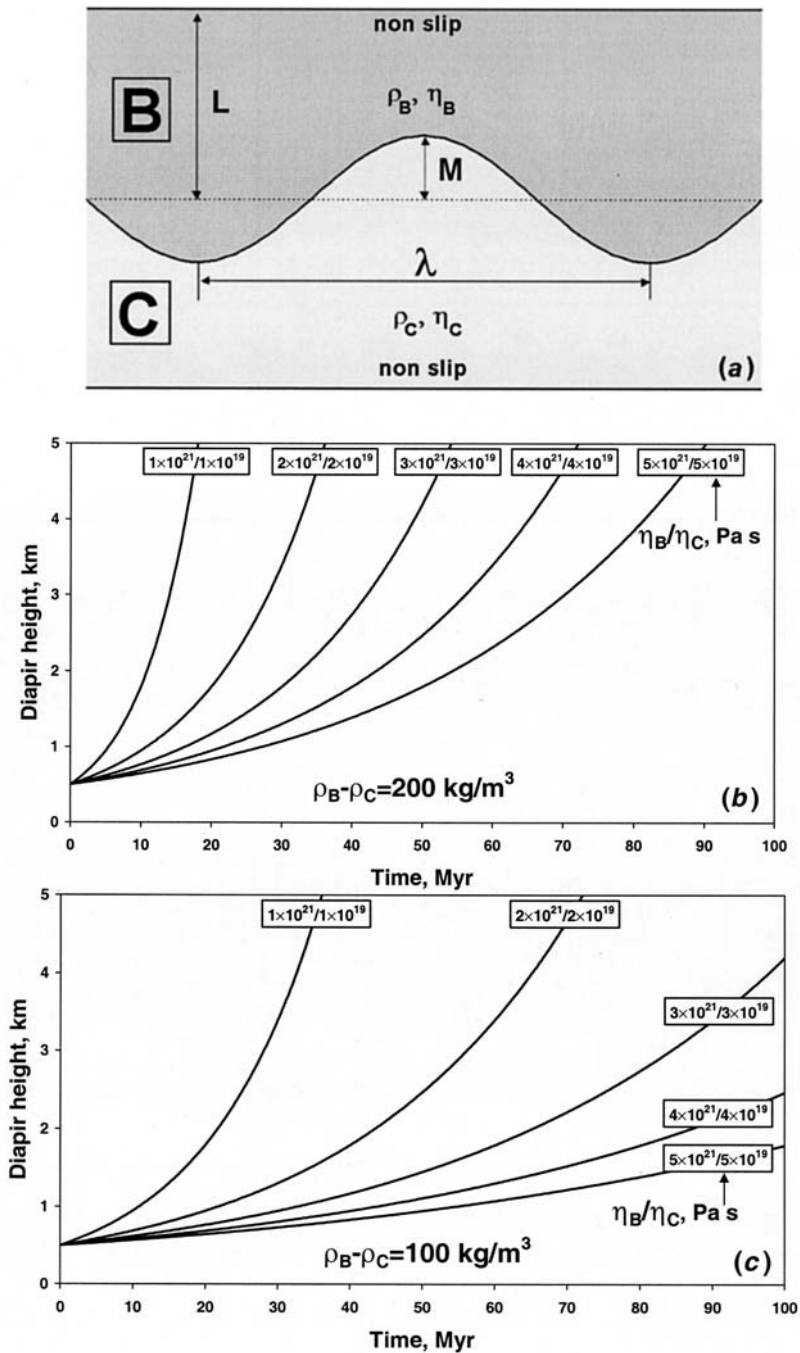


Fig. 9. Diapir growth for a two-layered model (Ramberg, 1981) representing layers B and C in Fig. 7 and 8. The initial design of the model and the boundary conditions are shown in (a); for further details see text. The height of a diapir as a function of time, calculated using equation (8), is shown for different density contrasts between layer B and C (see Fig. 7a).

Equation 6 were taken from the summary by Ranalli (1995). In our calculation we used a low value of  $10^{-15} \text{ s}^{-1}$  for the strain rate (e.g., Carter & Tsenn, 1987; Ranalli, 1995), in accordance with the assumption of active late-orogenic crustal deformation (e.g., Babeyko & Sobolev, 2001; and discussion below). From Fig. 7b it follows that the two lower layers C and D of the double-stacked crust are characterized by a strong ( $> 2$  orders of magnitude) decrease in viscosity, forming a rheologically weak zone (e.g., Carter & Tsenn, 1987; Ranalli, 1995). The lowest values of effective viscosity should characterize the buried

upper crust represented by layer C in Fig. 7 and 8, which is composed of quartz-rich granodioritic rocks and represents a buoyant body overthrust by denser and stiffer lower crustal rocks represented by layer B in Fig. 8. The low viscosity of this buoyant crust after thermal relaxation of the stacked crust should favor the activation of gravitational redistribution (Fig. 8) in the form of either crustal diapirism (e.g. Ramberg, 1981; Perchuk, 1989; Perchuk *et al.*, 1992, 1999; Gerya *et al.*, 2000b, 2001) or buoyant escape (squeezing) of the buried crust (e.g., Chemenda *et al.*, 1995; Arnold *et al.*, 2001).

Arnold *et al.* (2001) recently studied the late-orogenic evolution of a double-stacked crust underplated by hot asthenospheric mantle with two-dimensional thermomechanical numerical modeling experiments. The results show that in the absence of erosion and external tectonic forces partial melting and ductile rebound of the lower crust should be the dominant processes. Although buoyancy forces are present in the partially molten lower crust, the viscosity of the overburden is too high to allow diapiric ascent (Arnold *et al.*, 2001). On the other hand, the study of Babeyko & Sobolev (2001) shows that intense crustal convection can be triggered during relatively slow tectonic shortening of continental crust. This indicates that external tectonic forces can lead to — and may be necessary for — critical weakening of the crust (*e.g.*, along fault zones) to trigger processes of gravitational redistribution during late-orogenic evolution. In this case, strain localization by erosion (Ellis *et al.*, 2001) may also play a significant role in the exhumation of buoyant lower crustal rocks.

During gravitational redistribution the strain rate will vary significantly in space and time (*e.g.*, Bittner & Schmeling, 1995), thus influencing the effective viscosity of the rocks. Therefore, the viscosity profiles of Fig. 7b can only be representative for the very initial stage of the process if external tectonic forces uniformly affect the entire vertical section of the stacked crust. Nevertheless, it can be argued that the high ( $10^1 - 10^4$ ) viscosity contrast between the buried upper-crustal layer C in Fig. 7 and 8 and the overthrust lower-crustal layer B should be characteristic for late-orogenic stages during thermal relaxation (Fig. 6a). In this case, the development of crustal-scale gravitational redistribution is controlled (*e.g.*, Ramberg, 1981) by the absolute effective viscosity of the stronger, overthrust lower crustal rocks of layer B.

We used the diapiric model (Fig. 9a) of Ramberg (1981) in order to estimate semi-quantitatively the possible range of the effective viscosity of the overthrust lower crust of layer B which would allow the triggering of diapiric uprising of the buried upper crustal layer C (Fig. 7, 8). We note that layers B and C in Fig. 7 and 8 constitute an inversion of the distribution of density and viscosity with depth (Fig. 7), with a sharp discontinuity at the layer boundary. We assume that an initial sinusoidal disturbance of this boundary between the two layers has a small amplitude,  $M$ , and a characteristic wave length,  $\lambda$  (Ramberg, 1981). Thus the conditions to investigate the growth of a diapir are defined by the equation (Ramberg, 1981)

$$y(t) = M \exp[t \cdot (\rho_B - \rho_C) \cdot K \cdot L \cdot g / (2\eta_C)], \quad (8)$$

where  $y$  is the height of the diapir (m) as a function of time  $t$  (s);  $L$  is the thickness of each layer, m;  $\rho_B$  and  $\rho_C$  are the densities of layers B and C, respectively;  $\eta_C$  is the viscosity of the layer C, Pa·s;  $K$  is the factor of growth (Ramberg, 1981), dependent on the viscosity contrast. From Table 1 and Fig. 6 we assume  $L = 12,500$  m,  $\rho_B - \rho_C = 100 - 200$  kg/m<sup>3</sup> and  $M = 500$  m. Based on the calculated variations of viscosity with depth (Fig. 7b), we use a viscosity contrast of  $\eta_B/\eta_C = 10^2$  to estimate  $K = 0.0033$  (Ramberg, 1981). Figures 9b and 9c show the height of the resulting

diapir as a function of time for different values of  $\rho_B - \rho_C$  and  $\eta_B, \eta_C$ . According to these results, gravitational redistribution should proceed in realistic time scales of 10–100 Myr, comparable to those of thermal relaxation (Fig. 6), for a viscosity of the overthrust lower crust on the order of  $n \times 10^{21}$  Pa·s. Such significant lowering of the viscosity can be related to localized tectonic weakening of the crust (*e.g.*, along crustal-scale fault zones characterized by high pore-fluid pressure). The onset of the processes of gravitational redistribution within a stacked crust may thus be expected some tens of Myr after the beginning of thermal relaxation, when a high negative density contrast (Fig. 7a) related to prograde metamorphic phase transformations (Fig. 5) and a low effective viscosity of the buried crust (Fig. 7b) are attained.

## Conclusions

On the basis of our calculations it can be concluded that multilayered crustal structures created either by collision or by large-scale magmatic activity can be subjected to gravitational redistribution during the thermal relaxation of the stacked crust. The initiation of gravitational redistribution requires a decrease of effective rock viscosities to about  $n \times 10^{21}$  Pa·s or less. This can be achieved by an increase in temperature, by the application of external tectonic forces and possibly also by fluid/melt influx during the thermal relaxation of the stacked crust. Buoyant escape or extrusion ("squeezing") of buried upper crust (*e.g.*, Arnold *et al.*, 2001) can proceed *via* a weak low-viscosity "channel" formed by the buried upper crust itself (Fig. 8). This particular process has also been suggested to be an important feature during collision and associated normal faulting (*e.g.*, Chemenda *et al.*, 1995). If weak tectonic zones exist within the overthrust lower crust, gravitational redistribution in the form of crustal diapirism may occur within a < 100 Myr time interval, as interpolated from Fig. 9. For example, Gerya *et al.* (2000b) used two-dimensional numerical modeling of gravitational redistribution to analyze the shapes of exhumation  $P$ - $T$  paths in granulites from the Limpopo high-grade terrain of South Africa, for which collisional-type tectonic models had previously been suggested (*e.g.*, Roering *et al.*, 1992; De Wit *et al.*, 1992). The effective viscosity of the granulites and overlying lower-grade rocks during gravitational redistribution was estimated to be close to  $10^{19}$  Pa·s and  $10^{21}$  Pa·s, respectively, and these authors concluded that ~15 km of buoyant uplift of medium-pressure (7–8 kbar) granulites had occurred within about 9 Myr along a weak tectonic zone.

The strong correlation between the degree of gravitational instability and the calculated steady-state temperature in the lower part of the continental crust suggests that a gravitationally unstable crust will logically lead to further modifications, with a positive feed-back effect on gravitational redistribution. Higher geotherms will trigger prograde changes in mineral assemblages, leading to a further enhancement of vertical density inversions (Fig. 7a, see also Gerya *et al.*, 2001), or, given suitable water fugacities, to the generation of granitic magmas and low-

viscosity, partially molten zones in the lower part of the stacked crust (e.g., Belousov, 1989; Perchuk, 1989, 1991; Perchuk *et al.*, 1992, 1999, 2000a, b; Weinberg & Schmeling, 1992; Dirks, 1995; Bittner & Schmeling, 1995; Gerya *et al.*, 2000a and b; 2001; Arnold *et al.*, 2001). Gravitational redistribution should not only lead to a decrease in gravitational energy, and, as a result, to a more stable structure of the crust, but should also favour a final structure in which abundant basic, low-heat-productivity and high-density rocks should predominate in the lower part of this crust.

As noted above, gravitationally unstable crust may be produced in any large-scale process leading to inverted rock-density stratifications. Redistribution processes in such crust may play a significant role in the heat distribution during the formation of Precambrian granite-greenstone terrains (e.g., MacGregor, 1951; Ramberg, 1981) and spatially related granulite complexes (e.g., Perchuk, 1989, 1991; Perchuk *et al.*, 1992, 1999, 2000a and b), where the instability is produced by abundant mafic and ultramafic rocks of greenstone belts overlying sialic basement. However, gravitationally unstable crust is expected to result, above all, from collisional events involving initially stable sections of continental crust, where regional thrusting, multiple stacking and regional folding occur (e.g., the double-stacked crust of England & Thompson, 1984; Le Pichon *et al.*, 1997). This suggests a strong causal and temporal link between external collisional and internal gravitational mechanisms of rock deformation in high-grade metamorphic regions. Collisional mechanisms should operate during the early prograde stages of a tectonometamorphic cycle, causing thickening of the crust and a corresponding increase in radiogenic thermal supply, whereas gravitational mechanisms should dominate during the later thermal peak and retrograde stages, providing an important factor for the exhumation of high-grade rocks.

**Acknowledgements:** This work was carried out as part of a Russian-South African-German scientific collaboration project and supported by RFBR grants # 00-05-64939 to TVG, and #00-15-98520 as well as #99-05-65602 to LLP, by FRD and Gencor grants to DDVR, and by an Alexander von Humboldt Foundation Research Fellowship to TVG. We also acknowledge support by the Deutsche Forschungsgemeinschaft through SFB 526. The authors are grateful to anonymous reviewers for their valuable suggestions, resulting in substantial improvements to the manuscript.

## References

- Arnold, J., Jacoby, W.R., Schmeling, H., Schott, B. (2001): Continental collision and the dynamic and thermal evolution of the Variscan orogenic crustal root – numerical models, *J. Geodynamics*, **31**, 273-291.
- Babeyko, A. & Sobolev, S. (2001): Large-scale convection in the lower crust induced by tectonic shortening: rheological perspective. *Ber. Dtsch. Min. Ges. Beih. z. Eur. J. Mineral.*, **13**, 18.
- Belousov, V.V. (1989): Geotectonics. Nedra Press, Moscow, 381 p. (in Russian).
- Bittner, D. & Schmeling, H. (1995): Numerical modeling of melting processes and induced diapirism in the lower crust. *Geophys. J. International*, **123**, 59-70.
- Brace, W.F. (1980): Limits on lithospheric stress imposed by laboratory experiments. *J. Geophys. Res.*, **85**, 6248-6252.
- Buntebarth, G. (1991): Thermal model of cooling. in "Equilibrium and Kinetics in contact metamorphism", G. Voll, J. Topel, D.R.M. Pattison, F. Seifert, eds. Springer Verlag, Berlin, 379-402.
- Carter, N.L. & Tsenn, M.C. (1987): Flow properties of continental lithosphere. *Tectonophysics*, **136**, 27-63.
- Chemenda, A.I., Mattauer, M., Malavieille, J., Bokun, A.N. (1995): A mechanism for syn-collisional deep rock exhumation and associated normal faulting: Results from physical modeling. *Earth Planet Sci. Lett.*, **132**, 225-232.
- Clauser, C. & Huenges, E. (1995): Thermal conductivity of rocks and minerals. In: "Rock Physics and Phase Relations", T.J. Ahrens ed., AGU Reference Shelf 3, AGU, Washington D.C., 105-126.
- Cloos, M. (1982): Flow melanges: numerical modeling and geological constraints in their origin in Franciscan subduction complex, California. *Geol. Soc. Am. Bull.*, **93**, 330-345.
- Dale, J., Holland, T.J.B., Powell, R. (2000): Hornblende-garnet-plagioclase thermobarometry: a natural assemblage calibration of the thermodynamics of hornblende. *Contrib. Mineral. Petrol.*, **140**, 353-362.
- De Wit, M.J. & Ashwal, L.D. (1997): Greenstone Belts. Clarendon Press, Oxford, 1234 p.
- De Wit, M.J., Roering, C., Hart, R.J., Armstrong, R.A., De Ronde, C.J., Green, R.W.E., Tredoux, M., Pederdy, E., Hart, R.A. (1992): Formation of an Archean continent. *Nature*, **357**, 553-562.
- Dirks, P.H.G.M. (1995): Crustal convection: evidence from granulite terrains. Centennial Geocongress, Extended Abstracts, Geol. Soc. South Africa., 673-676.
- Ellis, S., Beaumont, C., Pfiffner, A. (1999): Geodynamic models of crustal-scale episodic tectonic accretion and underplating in subduction zones. *J. Geophys. Research*, **104**, 15169-15190.
- Ellis, S., Wissing, S., Beaumont, C., Pfiffner, A. (2001): Strain localisation as a key to reconciling experimentally derived flow-law data with dynamic models of continental collision. *Int. J. Earth Sci. (Geol. Rundsch.)*, **90**, 168-180.
- England, P.C. & Thompson, A.B. (1984): Pressure-temperature-time paths of regional metamorphism; I, Heat transfer during the evolution of regions of thickened continental crust. *J. Petrol.*, **25**, 894-928.
- , — (1986): Some thermal and tectonic models for crustal melting in continental collision zones. in "Collision Tectonics" M.P. Coward & A.C. Ries, eds. Geol. Soc. London, Spec. Publ., **19**, 83-94.
- Gerya, T.V., Perchuk, L.L., Maresch, W.V., Van Reenen, D.D., Smit, C.A., Willner A.P. (2000a): Numerical modeling of the exhumation of Precambrian granulite facies terrains. *Ber. Dtsch. Min. Ges. Beih. z. Eur. J. Mineral.*, **12**, 59.
- Gerya, T.V., Perchuk, L.L., Van Reenen, D.D., Smit, C.A. (2000b): Two-dimensional numerical modeling of pressure-temperature-time paths for the exhumation of some granulite facies terrains in the Precambrian. *J. Geodynamics*, **30**, 17-35.
- Gerya, T.V., Maresch, W.V., Willner A.P., Van Reenen, D.D., Smit, C.A. (2001): Inherent gravitational instability of thickened continental crust with regionally developed low- to medium-



- pressure granulite facies metamorphism. *Earth Planet. Sci. Lett.*, **190**, 221-235.
- Henry, P., Le Pichon, X., Goffé, B. (1997): Kinematic, thermal and petrological model of the Himalayas: constraints related to metamorphism within the und thrust Indian crust and topographic elevation. *Tectonophysics*, **273**, 31-56.
- Holland, T.J.B. & Powell, R. (1998): Internally consistent thermodynamic data set for phases of petrological interest. *J. metamorphic Geol.*, **16**, 309-344.
- Holland, T.J.B., Baker, J., Powell, R. (1998): Mixing properties and activity-composition relationships of chlorites in the system MgO-FeO-Al<sub>2</sub>O<sub>3</sub>-SiO<sub>2</sub>-H<sub>2</sub>O. *Eur. J. Mineral.*, **10**, 395-406.
- Kretz, R. (1983): Symbols for rock-forming minerals. *Am. Mineral.*, **68**, 277-279.
- Krohe, A. (1998): Extending a thickened crustal bulge: toward a new geodynamic evolution model of the paleozoic NW Bohemian Massif, German Continental Deep Drilling site (SE Germany). *Earth-Sci. Rev.*, **44**, 95-145.
- Le Pichon, X., Henry, P., Goffé, B. (1997): Uplift of Tibet: from eclogites to granulites – implications for the Andean Plateau and the Variscan belt. *Tectonophysics*, **273**, 57-76.
- MacGregor, A.M. (1951): Some milestones in the Precambrian of Southern Rhodesia. *Transact. Geol. Soc. South Africa*, **54**, 27-71.
- McLennan, S. (1992): Continental crust. *Encycl. Earth Sci.*, **1**, 1085-1098.
- Midgley, J.P. & Blundell, D.J. (1997): Deep seismic structure and thermo-mechanical modeling of continental collision zones. *Tectonophysics*, **273**, 155-167.
- Perchuk, L.L. (1989): P-T-fluid regimes of metamorphism and related magmatism with specific reference to the Baikal Lake granulites. in "Evolution of Metamorphic Belts", S. Daly, D.W.D. Yardley, B. Cliff, eds. Geol. Soc. London, Spec. Publ., 275-291.
- (1991): Studies in magmatism, metamorphism and geodynamics. *International Geol. Rev.*, **33**, 311-374.
- Perchuk, L.L., Podladchikov, Y.Y., Polaykov, A.N. (1992): P-T paths and geodynamic modelling some metamorphic processes. *J. metamorphic Geol.*, **10**, 311-319.
- Perchuk, L.L., Gerya, T.V., Van Reenen, D.D., Safonov, O.G., Smit, C.A. (1996): The Limpopo metamorphic complex, South Africa: 2. Decompression/cooling regimes of granulites and adjusted rocks of the Kaapvaal craton. *Petrology*, **4**, 571-599.
- Perchuk, L.L., Krotov, A.V., Gerya, T.V. (1999): Petrology of amphibolites of the Tanaelv Belt and granulites of the Lapland complex. *Petrology*, **7**, 539-563.
- Perchuk, L.L., Gerya, T.V., Van Reenen, D.D., Krotov, A.V., Safonov, O.G., Smit, C.A., Shur, M.Y. (2000a): Comparable petrology and metamorphic evolution of the Limpopo (South Africa) and Lapland (Fennoscandia) high-grade terrains. *Mineral. Petrol.*, **69**, 69-107.
- Perchuk, L.L., Gerya, T.V., Van Reenen, D.D., Smit, C.A., Krotov, A.V. (2000b): P-T paths and tectonic evolution of shear zones separating high-grade terrains from cratons: examples from Kola Peninsula (Russia) and Limpopo region (South Africa). *Mineral. Petrol.*, **69**, 109-142.
- Powell, R. & Holland, T.J.B. (1999): Relating formulations of the thermodynamics of mineral solid solutions: Activity modeling of pyroxenes, amphiboles, and micas. *Am. Mineral.*, **84**, 1-14.
- Ramberg, H. (1981): Gravity, Deformation and Geological Application. Academic Press, London, NY, San Francisco, 452 p.
- Ranalli, G. (1995): Rheology of the Earth, 2nd ed. Chapman and Hall, London, 413 p.
- Roering, C., van Reenen, D.D., Smit, C.A., Barton, J.M. Jr., de Beer, J.H., De Wit, M.J., Stettler, E.H., Van Schalkwyk, J.F., Stevens, G., Pretorius, S. (1992): Tectonic model for the evolution of the Limpopo Belt. *Precamb. Res.*, **55**, 539-552.
- Ruppel, C. & Hodges, K.V. (1994): Role of horizontal thermal conduction and finite time thrust emplacement in simulation of pressure-temperature-time paths. *Earth Planet. Sci. Lett.*, **123**, 49-60.
- Shemenda, A.I. (1993): Subduction of the lithosphere and back arc dynamics: insights from physical modeling. *J. Geophys. Res.*, **98**, 16167-16185.
- Shi, Y. & Wang, C. (1987): Two-dimensional modeling of the P-T paths of regional metamorphism in simple overthrust terrains. *Geology*, **15**, 1048-1051.
- Schott, B. & Schmeling, H. (1998): Delamination and detachment of a lithospheric root. *Tectonophysics*, **296**, 225-247.
- Turcotte, D.L. & Schubert, G. (1982): Geodynamics: Applications of Continuum Physics to Geological Problems. John Wiley, NY, 450 p.
- Weinberg, R.B. & Schmeling, H. (1992): Polydiapirs: multiwavelength gravity structures. *J. Structural Geol.*, **14**, 425-436.
- Willner, A.P., Sebazungu, E., Gerya, T.V., Maresch, V.W., Krohe, A. (2002): Numerical modelling of PT-paths related to rapid exhumation of high-pressure rocks from the crustal root in the Variscan Erzgebirge Dome (Saxony/Germany). *J. Geodynamics*, (in press).
- Yardley, B.W.D. (1989): An Introduction to Metamorphic Petrology. Earth Science series, Longman, Singapore, 248 p.

Received 20 June 2001

Modified version received 21 December 2001

Accepted 12 February 2002